Developmental Cell, Vol. 7, 387–399, September, 2004, Copyright ©2004 by Cell Press

Invasive Cell Behavior during *Drosophila* Imaginal Disc Eversion Is Mediated by the JNK Signaling Cascade

José Carlos Pastor-Pareja,[1,2] Ferdinand Grawe,[3] Enrique Martín-Blanco,[2,*] and Antonio García-Bellido[1]

[1]Centro de Biología Molecular "Severo Ochoa"
CSIC-UAM
Cantoblanco
28049 Madrid
Spain

[2]Institut de Biologia Molecular de Barcelona
CSIC
Parc Científic de Barcelona
Josep Samitier 1-5
08028 Barcelona
Spain

[3]Institut für Genetik
Heinrich-Heine Universität Düsseldorf
Universitätstrasse 1
D-40225 Düsseldorf
Germany

Summary

***Drosophila* imaginal discs are monolayered epithelial invaginations that grow during larval stages and evert at metamorphosis to assemble the adult exoskeleton. They consist of columnar cells, forming the imaginal epithelium, as well as squamous cells, which constitute the peripodial epithelium and stalk (PS). Here, we uncover a new morphogenetic/cellular mechanism for disc eversion. We show that imaginal discs evert by apposing their peripodial side to the larval epidermis and through the invasion of the larval epidermis by PS cells, which undergo a pseudo-epithelial-mesenchymal transition (PEMT). As a consequence, the PS/larval bilayer is perforated and the imaginal epithelia protrude, a process reminiscent of other developmental events, such as epithelial perforation in chordates. When eversion is completed, PS cells localize to the leading front, heading disc expansion. We found that the JNK pathway is necessary for PS/larval cells apposition, the PEMT, and the motile activity of leading front cells.**

Introduction

During development, epithelial cells associate in polarized sheets, which undergo morphogenetic remodeling resulting from modifications in the relative position of the cells, localized cell proliferation, cell death, and changes in cell shape. Most of these processes directly or indirectly depend on the coordinated control of cell attraction, repulsion, and differential adhesion, and on the intracellular forces generated by the cell cytoskeleton.

One of the processes that best exemplify the dramatic changes that shape organisms is insect metamorphosis. In *Drosophila* and other holometabolous insects, most of the larval structures are replaced with new tissues that will give rise to the adult or *imago*. In particular, the adult epidermis with the exception of the abdominal structures develops from imaginal epithelial discs. During larval stages, the primordia of imaginal discs, set during embryogenesis, invaginate and grow to become flattened sacs arranged in a monolayer epithelium connected to the larval epidermis by a stalk. The mature discs contain two populations of cells, a columnar epithelium that will give rise to most of the adult structures and a thinner and more squamous peripodial epithelium (PE) with a reduced contribution to adult tissues. Upon metamorphosis, the imaginal discs undergo striking morphological changes, everting, expanding, and fusing to ipsilateral and contralateral adjacent discs generating the adult exoskeleton (Fristrom and Fristrom, 1993).

The process of movement and sealing of imaginal discs and, in general, epithelial sheets can be subdivided into three sequential steps: (1) leading cells are specified and brought into position; (2) cells execute coordinated forward movements by changing shape and/or migrating over a substratum; and (3) sheets merge and fuse. Most recent work on disc morphogenesis has focused on the cellular and molecular events underlying their late expansion and fusion (reviewed in Martín-Blanco and Knust, 2001), while the mechanisms involved in disc eversion have been poorly explored in vivo.

In late third instar larvae, the steroid molting hormone 20-hydroxyecdysone is believed to coordinate the almost simultaneous eversion of all discs by inducing a contraction of the PE. This is thought to drive movement of the appendages to the outside of the larval epidermis through relaxed and widened disc stalks (Poodry and Schneiderman, 1970). This classical view is supported by in vitro studies showing that treatment of cultured discs with ecdysone is sufficient to induce eversion (Milner, 1977) and that contraction of an intact PE is necessary to achieve this goal (Milner et al., 1984). These and other descriptive reports (Mandaron and Guillermet, 1978; Usui and Simpson, 2000) have led to the textbook proposition that cell shape changes (longitudinal contraction in the PE and circumferential elongation at the disc stalks) are sufficient for imaginal disc eversion (Wolpert et al., 2002). However, there are as yet no data to confirm that this mechanism exists in vivo and no convincing explanation on how a stalk of no more than ten cells in diameter could achieve the width required to allow the entire disc (more than 60,000 cells) to pass through. Further, this accepted view neglects earlier proposals suggesting a different eversion mechanism mediated by the rupture of the PE (Waddington, 1941; Auerbach, 1936). A model supported by fate maps developed for the PE of *Calliphora*, a related dipteran, imaginal wing discs (Sprey and Oldenhave, 1974).

Several studies have revealed a requirement for cytoskeletal components and a number of signal transduction molecules for imaginal disc morphogenesis during the first hours of metamorphosis. The latter include the *Drosophila* AP-1 transcription factors, D-Jun and D-Fos

*Correspondence: embbmc@cid.csic.es

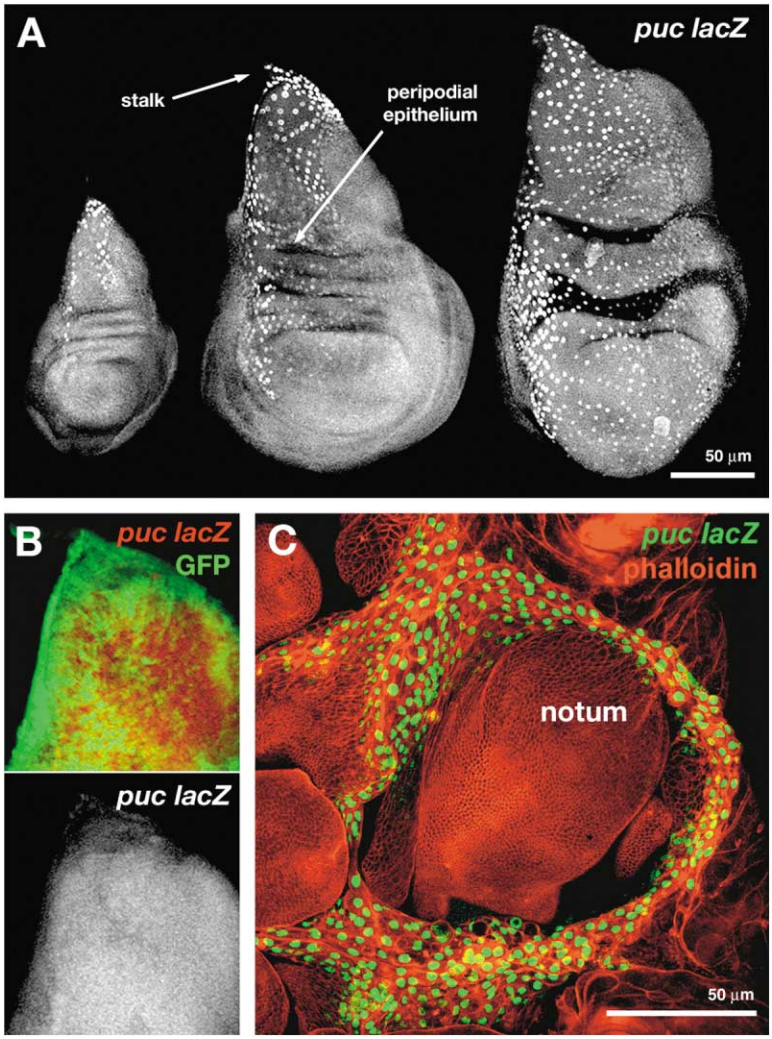

Figure 1. JNK Signaling Is Active in Peripodial and Stalk Cells prior to and at Eversion

(A) *puckered* expression in wing imaginal discs before eversion. *puc* is expressed in the stalk of the disc throughout the third larval stage and in an increasing number of PE cells as larva ages. At the end of the third larval instar, the entire PE expresses *puc*. *puc* is detected by anti-β-gal staining in the puc^{E69} lacZ enhancer trap line.

(B) Puc ubiquitous expression, driven by actin-GAL4 (see Experimental Procedures), represses JNK signaling in the PS cells of larval wing discs. puc^{E69} β-gal expression (red and lower panel) induced by JNK activity is abolished upon expression of *Puc* (visualized by GFP coexpression). Same effects on *puc* expression can be seen in *hep* (D-JNKK) mutant discs (Martín-Blanco et al., 2000, and data not shown)

(C) *puc* expression is restricted to cells at the edge of a half-everted wing imaginal disc in a wild-type pupa 4.5 hr APF. At this time, more than 70% of *puc* expressing cells are present at the leading front. Puc is revealed by puc^{E69} β-gal expression (green). Actin (phalloidin) staining is shown in red.

(Kayak [Kay]) (Zeitlinger and Bohmann, 1999; Zeitlinger et al., 1997), and an upstream kinase cascade homologous to the Jun-NH2-terminal kinase (JNK) pathway in mammals. The core of this cascade is formed by the stress-activated kinases JNKK and JNK. In *Drosophila*, JNKK and JNK homologs are encoded by the genes *hemipterous* (*hep*) (Glise et al., 1995) and *basket* (*bsk)* (Riesgo-Escovar et al., 1996). JNK signaling mutant larvae do not spread their discs in the process of thorax closure (Agnes et al., 1999; Martín-Blanco et al., 2000; Noselli and Agnes, 1999; Suzanne et al., 2001; Tateno et al., 2000; Zeitlinger and Bohmann, 1999). This phenotype is accompanied by a loss of *puckered (puc)* expression in the disc stalk and the PE (Agnes et al., 1999). Puc is a dual-specificity phosphatase that selectively inactivates Bsk and, thus, is thought to act in a negative feedback loop (Martín-Blanco et al., 1998). JNK activity is necessary to maintain the adhesion of the imaginal leading edge cells to their larval substrate and to promote actin dynamics (lamellipodia and filopodia formation) (Martín-Blanco et al., 2000). It has been shown that this signaling cascade also regulates the process of embryonic dorsal closure, where the embryonic epidermis fuses along the dorsal midline (reviewed in Martín-Blanco, 1997; Noselli, 1998). Based on these similarities, it has been suggested that a conserved mechanism regulates the spreading and fusion of epithelial sheets.

In this paper, we uncover a new morphogenetic/cellular mechanism for disc eversion based on histological sections and direct observation of imaginal morphogenesis in vivo. We found that, at the onset of metamorphosis, imaginal discs coordinately appose their peripodial sides and stalks (PS cells) to the larval epidermis. Then, eversion proceeds through the progressive invasion of the larval epidermis by PS cells undergoing a pseudoepithelial-mesenchymal transition (PEMT). Multiple perforations in the peripodial/larval bilayer are thus generated, which coalesce with the disc stalk into a single hole, widening the gap and allowing disc evagination. When eversion is complete, the PS cells localize to the leading front of the discs, spearheading their expansion over larval cells. We also analyze the roles of the JNK pathway at discrete steps of disc morphogenesis progression. We demonstrate that the JNK cascade functions to promote the apposition of PS and larval cells,

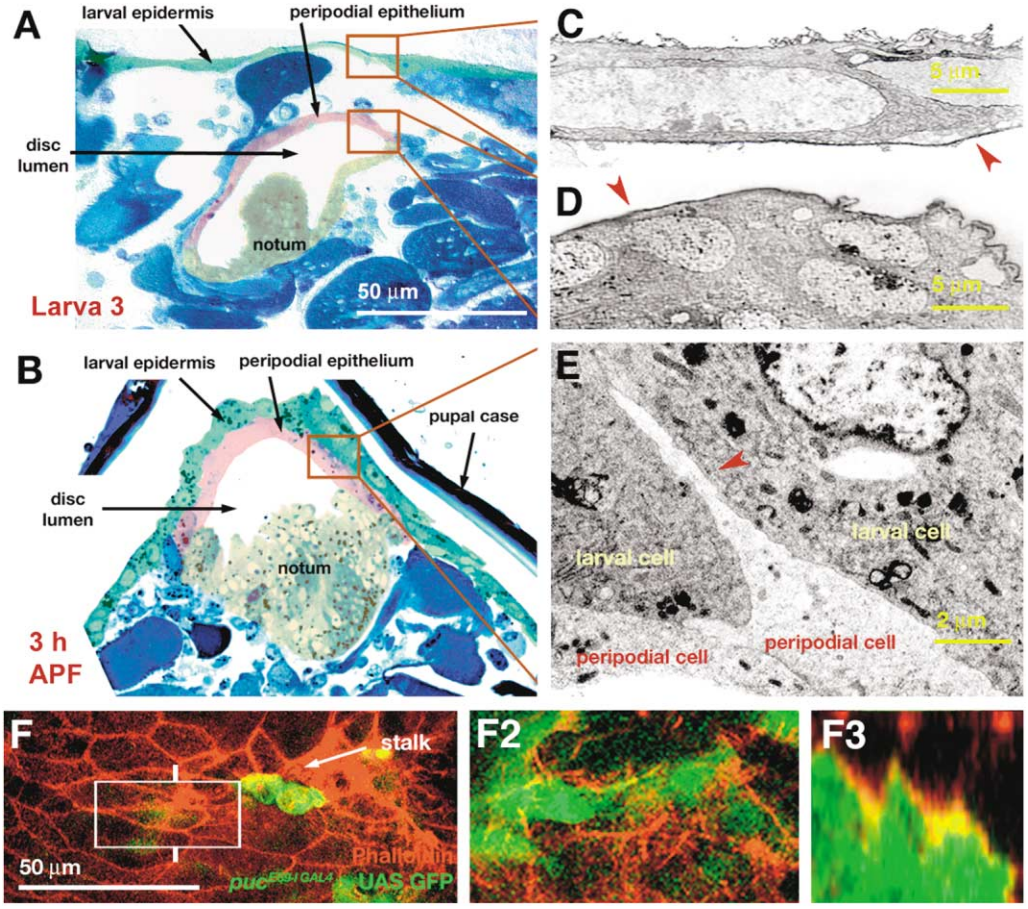

Figure 2. Peripodial and Stalk Cells Invade the Larval Epidermis at the Onset of Disc Eversion

(A) Semithin transverse section of a white prepupa. The notum of the wing imaginal disc does not contact the larval epidermis (except for the stalk in a different section; not shown). Larval muscles and trachea remain in place under the larval epithelia. The different epithelial layers have been colored to facilitate visualization: green, larval cells; pink, PS cells; yellow, imaginal cells. Insets depict the location and orientation of (C) and (D).

(B) Semithin transversal section of a 3 hr APF pupa showing adhesion between PS and larval epidermal cells at the level of the notum. This adhesion involves a basal-basal contact of the two epidermal layers. Color-code as in (A). Inset depicts the location and orientation of (E).

(C and D) The basal lamina (arrowheads) is present at the basal surface of larval epithelial cells (C) and at the basal (external) surface of imaginal discs (D) (ultrathin electron microscope section).

(E) The basal lamina is absent between PS and larval cells (ultrathin electron microscope section). The PS cells begin to intercalate into the larval layer (arrowhead).

(F) Confocal section at the larval epidermal surface showing the position of insertion of the stalk (*puc*-expressing cells) of a wing imaginal disc 2.5 hr APF. (F2) Magnification of the inset in (F) in a lower focal plane under the larval epidermis. The *puc*-expressing PS cells show actin-rich basal protrusions interdigitating into the larval epidermis (arrowhead). (F3) Z axis section at the level of the white lateral marks in the inset area, showing *puc*-expressing cells basal projections. Phalloidin (actin) is stained in red. *puc*-expressing cells are green (GFP-expressing $puc^{E69\text{-}I\ GAL4}$).

to determine the degree of PEMT and the motility of leading edge/PS cells, and to maintain the adhesion between the larval and imaginal tissue. We propose that this molecular mechanism can be relevant to morphogenetic processes of perforation of transient epithelia in different phyla.

Results

The Eversion of Imaginal Discs: A Topological Problem

The current view of imaginal disc eversion asserts that the externalization of appendage primordia proceed through widened discs' stalks during early pupal development (Fristrom and Fristrom, 1993). However, a detailed analysis of PS cell markers appears to challenge this simple inversion mechanism.

In early third instar imaginal wing discs, we observed that the gene *puc* was expressed at high levels in stalk cells and some PE cells (Figure 1A, left). This expression evolves through the third instar (Figure 1A, middle) until all PS cells (about 700 in the mature wing disc) expressed *puc* at the white prepupa stage (0–1 hr hours after puparium formation [APF]) (Figure 1A, right). These dynamic changes of *puc* expression were also observed in leg, haltere, and eye discs. The PS expression of *puc*

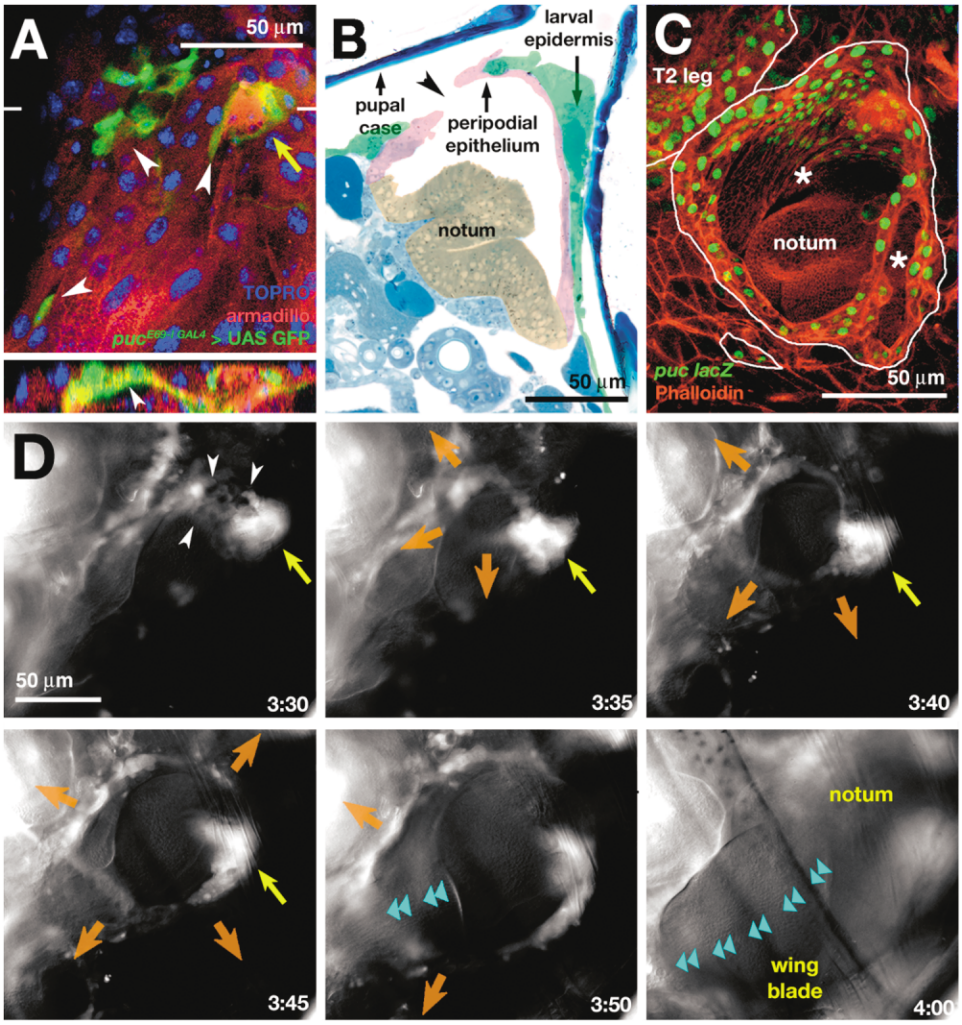

Figure 3. Cell Intercalation and Perforation of the Larval/Peripodial Bilayer

(A) Confocal section at the larval epidermal surface showing substitution of larval epidermal cells by *puc*-expressing PS cells in multiple locations (arrowheads) (see also Z axis section in the lower panel at the level of the white lateral marks). A thin yellow arrow marks the position of the disc stalk. *puc*-expressing cells are green (GFP-expressing $puc^{E69\text{-}I\ GAL4}$). Arm and TOPRO stainings are shown in red and blue, respectively.

(B) A semithin transversal section of a 3.5 hr APF pupa shows connection of the disc lumen with the space between the pupal case and the larval epidermis. Color-code as in Figure 2.

(C) Confocal projection of an everting wing imaginal disc (3 hr APF). The disc lumen opens up to the external surface under the pupal case through several holes (asterisks; two in this micrograph) generated by invasion of the larval tissue by *puc*-expressing PS cells (green). Actin (phalloidin) staining is shown in red.

(D) Snapshots from Supplemental Movie S1 showing the eversion process in a GFP-expressing $puc^{E69\text{-}I\ GAL4}$ pupa. The initial holes (arrowheads) coalesce into a single hole. The widening of the hole (thick arrows) occurs by intercalation of new cells at its edge and proceeds until all PS cells are located in a belt surrounding the everted disc. A thin arrow marks the position of the disc stalk. Serial arrowheads describe the eversion of the wing blade.

strictly depended on JNK activity, and it was abolished from mutant *hep* (JNKK) larvae (Agnes et al., 1999) or after Puc overexpression (Figure 1B). Thus, a JNK signaling feedback loop, first described during embryonic dorsal closure (Martín-Blanco et al., 1998), was shared by PS cells at the onset of the eversion and closure of the discs. During wing disc eversion, only cells found at the edge of the hole through which the disc everts (Figure 1C) and at the leading front mediating fusion to adjacent prothoracic, mesothoracic, and metathoracic discs (Agnes et al., 1999; Martín-Blanco et al., 2000; Usui and Simpson, 2000; Zeitlinger and Bohmann, 1999) showed *puc* expression, and hence JNK activity. Importantly, marking all cells that have expressed *puc* as well as their descendants showed that *puc*-expressing cells did not change their identity, nor did they die or get excluded from the epithelium until the end of the disc fusion process, when most of these cells were lost (Supplemental Figure S1 at http://www.developmentalcell.com/cgi/content/full/7/3/387/DC1). Hence, all PS cells are recruited to the front edge during disc eversion.

Our findings lead to a topological dilemma. In order

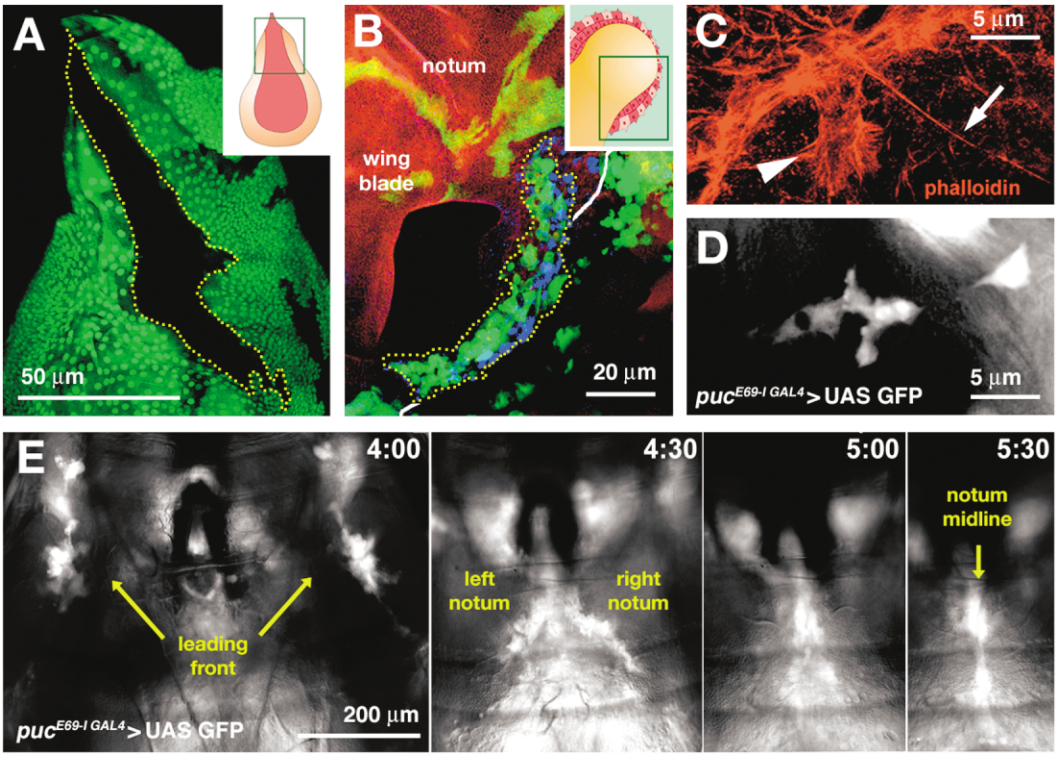

Figure 4. Intercalation and Motility in PS Cells

(A and B) Clonal analysis of wing imaginal discs PS cells (see Experimental Procedures).

(A) Clones (black) in the PE, as in the rest of the disc, are always compact in third instar larvae (dotted line).

(B) At 4 hr APF, clones (n = 14) at the leading front show cell intercalation. Thus, cells from the same lineage become separated and the cohesion of the clone is lost. The dotted line encloses a clone showing intercalation of *puc*-expressing cells. Actin (phalloidin) and the nuclei of *puc*-expressing cells are shown in red and blue, respectively. Insets in right inside corner diagrams describe the position and orientation of (A) and (B).

(C) Cells at the leading front emit lamellipodia (arrowhead) and long filopodia (arrow) in a 4.5 hr APF pupae (fixed tissue stained with phalloidin [filamentous actin]).

(D) Snapshot from Supplemental Movie S2 showing the motile activity of a GFP-expressing $puc^{E69\text{-}I\ GAL4}$ cell at disc eversion.

(E) Snapshots from Supplemental Movie S3 showing the closure of the wing discs at the dorsal midline in a GFP-expressing $puc^{E69\text{-}I\ GAL4}$ pupa. After eversion, PS cells become the leading front of the imaginal discs.

to reach their final position at the leading front, the PS cells would need to reposition themselves within the epithelia. Although this rearrangement just could be achieved through a massive constriction of the PE, we have uncovered a complementary mechanism, which involves larval epidermis perforation and PE cells intercalation.

Disc Eversion Proceeds throughout Invasion and Perforation of the Larval Epidermis and Planar Cell Intercalation of PS Cells

At third instar larval stages, the wing disc obliquely hangs from the larval epidermis, which is separated from the peripodial surface of the disc at the notum level by several larval muscles and tracheal tubules (Figure 2A). The disc and the larval epidermis are isolated by their corresponding extracellular basal lamina (Figures 2C and 2D). During late third instar stages and the first hours APF, the notum-wing side of the disc folds progressively to acquire the adult organ shape. We found that, at the initiation of pupariation, the disc affixes to the larval epidermis through its peripodial side. At 3 hr APF, the PS cells lose their squamous shape to adopt a more rounded one and are found in close contact with the larval epidermal cells via their basal surfaces (Figure 2B). Multiple actin-rich protrusions lead this apposition (Figure 2F). At this step, the basal lamina in between both layers degrades, leading to an intimate adhesion (Figure 2E).

Once imaginal discs appose the larval epidermis, we observed that PS cells, mostly around the disc stalk, invade the larval epithelium, gradually replacing the larval cells at the pupal surface without compromising the integrity of the peripodial sheet (Figure 3A). Several holes are opened in the peripodial/larval bilayer (Figures 3B, 3C, and 5B), which within a few minutes converge with the original stalk into a single aperture (Figure 3D and Supplemental Movie S1). Interfering with apoptosis by overexpressing the P35 cell death inhibitor in imaginal and larval tissues does not affect epithelial perforation and disc eversion (data not shown).

Following coalescence, we observed the progressive widening of the hole by intercalation of PS cells at the leading front (Supplemental Movies S1 and S2). We performed a cell lineage analysis and found that multiple clones of PS cells, which remain compact up to the third

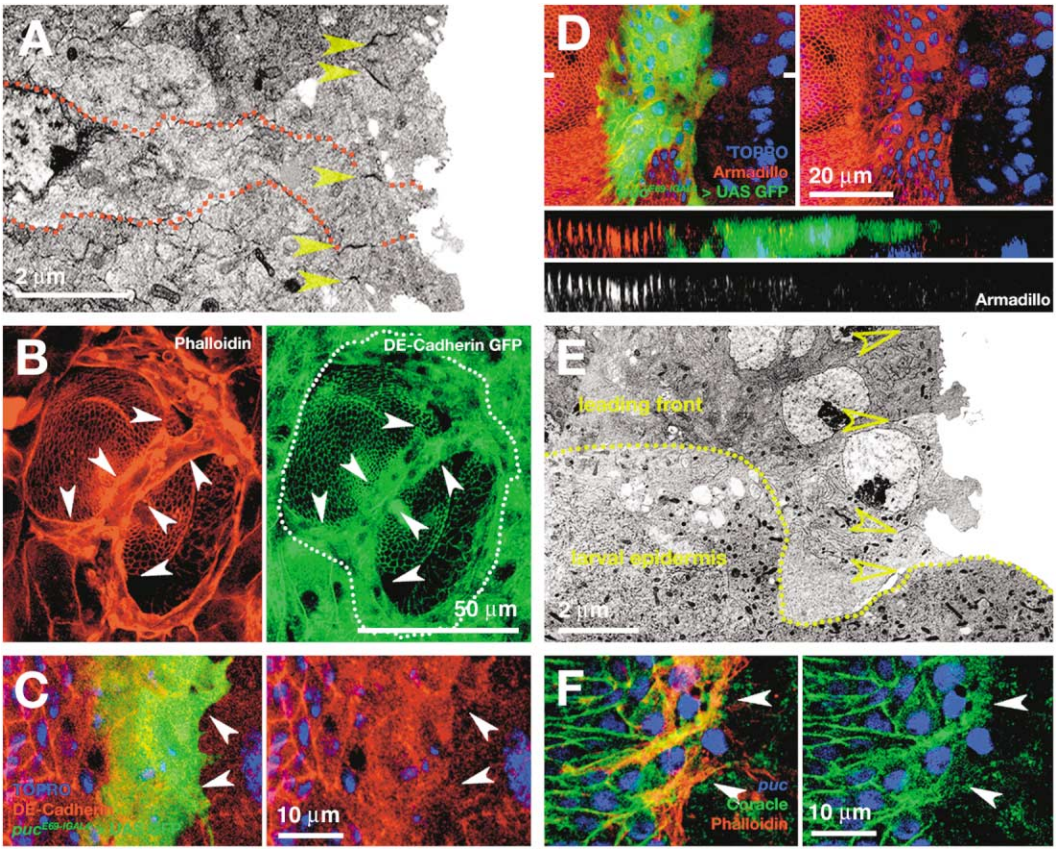

Figure 5. Cell-Cell Adhesion and Apico-Basal Polarity Are Lost in PS Cells during Eversion and in the Leading Front

(A) Transmission electron micrograph showing ZAs (arrowheads) in imaginal cells of a wing disc from a 4 hr APF pupae. The dotted line outlines the perimeter of an imaginal cell.

(B) Confocal projection of an everting wing imaginal disc (3.5 hr APF). DE-cadherin-GFP is ubiquitously expressed and localizes into the apical membranes (ZAs) of imaginal cells. Cells at the edges of the peripodial/larval holes show an accumulation of filamentous actin (phalloidin) in red. These same cells show a delocalization of DE-cadherin (green) into the cytoplasm (arrowheads).

(C) Confocal image of an expanding left wing imaginal disc (4.5 hr APF). DE-cadherin (red), a component of ZAs, relocates from the apical membrane (in imaginal cells) to the cytoplasm in *puc*-expressing leading front cells (GFP-expressing $puc^{E69\text{-}I\ GAL4}$). Arrowheads point to the edge of the leading front. TOPRO staining of nuclei is shown in blue.

(D) Confocal image of an expanding wing imaginal disc (4.5 hr APF). Arm (red) is excluded from apical cell membranes on *puc*-expressing leading front cells (GFP-expressing $puc^{E69\text{-}I\ GAL4}$) that disassemble their ZAs. A Z axis section shows the progressive disassembly of ZAs from cells in the proximity of the leading front. TOPRO staining of nuclei is shown in blue.

(E) Transmission electron micrograph of the leading front of a spreading imaginal wing disc (4.5 hr APF). ZAs are not present in cells of the leading front (arrowheads, compare with [A]). The dotted line outlines the contact between imaginal and larval cells.

(F) Confocal image of an expanding left wing imaginal disc (4.5 hr APF). Coracle, a component of subapical septate junctions, localizes to the cell membranes of imaginal discs but is excluded from the membrane and diffuses into the cytoplasm in cells at the leading front (green) expressing the puc^{E69} β-gal transgene (blue). Actin (phalloidin) staining is shown in red.

instar larval stage in the PE (Resino et al., 2002), lose cohesion during eversion (e.g., compare Figures 4A and 4B). Thus, PS cells appear to change neighbors, become extremely active, and emit and retract filopodia and lamellipodia at their front and rear ends (Figures 4C and 4D; Supplemental Movies S2 and S4). They squeeze in between themselves and the rest of the epithelium (planar intercalation), migrating to and expanding the front of the disc, and leading the migration over the larval tissue (Figure 4E; Supplemental Movie S3).

Simultaneous to wing disc eversion, all legs and haltere discs evert using the same mechanism (data not shown).

Disc Eversion Requires a Pseudo-Epithelial-Mesenchymal Transition of PS Cells

One hallmark of epithelial cells is their distinct apico-basal cell polarity. This polarity depends on a set of intercellular connections, which encircle epithelial cells at the border of the apical and basal-lateral membrane domains (reviewed in Knust and Bossinger, 2002). The cells in insect epithelial tissues are interconnected by zonula adherens (ZAs), which function in both cellular adhesion and signaling. DE-cadherin is the major constituent of the ZAs in a complex with Armadillo (Arm, β-catenin) and Dα-catenin. In addition, epithelia of flies and other invertebrates exhibit septate junctions, which

are located basally to the ZAs. Septate junctions prevent diffusion through the pericellular space and are functionally equivalent to vertebrate tight junctions.

All imaginal disc cells at the third instar larval stage presented ZAs (Figure 5A) in an apical belt. During disc eversion, however, we found that ZAs components delocalize from the free edges of the PS cells, remaining cytoplasmic at the edges of the perforations arising through the PS/larval bilayer (DE-cadherin, Figure 5B) and in those PS cells leading the spreading of the discs over the larval tissues (DE-cadherin, Figure 5C, and Arm, Figure 5D). As a consequence, we observed that ZAs were lost in these cells (Figure 5E). Moreover, septate junction components, such as Coracle (Figure 5F) and Disc Large (data not shown) were also found to be missing from the membranes of leading front cells.

The loss of apico/basal polarity and adhesion of the PS cells during disc eversion is reminiscent of an epithelial-mesenchymal transition (EMT), as described for mesoderm and neural crest cells in vertebrates, and for the acquisition of the invasive phenotype in carcinomas.

A Balanced Level of JNK Signaling Is Required at Different Steps of Disc Eversion and Closure

The JNK signaling cascade dictates the expression of *puc* in all PS cells but their early specification appears not to be affected by lowering the level of JNK activity, as the complete absence of Hep function did not alter either their number or morphology in third instar larval discs (data not shown). However, several mutant phenotypes have provided strong evidence for a leading role of the JNK pathway in imaginal disc fusion and disc eversion; e.g., *hep* mutants occasionally show uneverted wing discs lying inside the body of the pupa (Agnes et al., 1999). When and how is JNK signaling needed? Transversal semithin sections, at 6 $\pm$ 1 hr APF, long after closure is completed in wild-type, of hep^{r75} (a strong hypomorphic mutation) pupae show a range of phenotypic defects (classes I to III) (Figures 6A1–6A3). Class I corresponded to a complete failure of PS/larval apposition (40% of individuals); in class II, discs apposed to the larval tissue but did not complete their eversion (50%); the mildest condition, class III, refers to discs that everted completely and advanced to some extent but were unable to fuse (10%). By the complete inactivation of the JNK signaling cascade through the ubiquitous overexpression of *puc* (from 48–60 hr before puparium formation onward), we found a fully penetrant failure of disc apposition to the larval epidermis (class I phenotype) (Figure 6A and Table 1). A delayed or reduced (in a *puc* heterozygous background) overexpression of *puc* produced less severe class II and III phenotypes (Figures 6B and 6C and Table 1). Thus, the JNK cascade appears to be essential for PS and larval cell apposition and, as suggested by the observed phenotypic progression, may also be involved in later steps during eversion.

JNK activity levels also affect the degree of PEMT in PS cells. As described above, ZAs were absent from leading front cells and the membrane localization of DE-cadherin and Arm was progressively lost, as PS cells moved closer to the free edge (Figures 5C–5E). However, we found that in hep^{r75} mutant pupae (class III), the cells at the leading front of the disc did not delocalize either Arm or DE-cadherin in the free edge (Figures 6D and 6G), suggesting that partial loss of JNK signaling blocked the correct transition of these cells from immotile epithelial to migrating and invading leading front cells. Further, a surplus of JNK activity in PS cells in $puc^{E69F\text{-}GAL4}$ mutants conveyed the transition of an excess of PS cells to a mesenchymatic phenotype (Figures 6F and 6I, compare to Figures 6E and 6H [wild-type condition]). Hence, an adequate balance of JNK activity is key to control the level of PEMT. Too few mesenchymal-like PS cells restrained the ability of discs to evert and spread, while too many transformed cells affected the ability of discs to appropriately fuse (Figure 6J). Further, $puc^{E69F\text{-}GAL4}$ mutants also showed enhanced cell motility and massive cell detachment from the free edges of the epithelium. These cells adopted a rounded shape but remained in close proximity, establishing transient contacts (Supplemental Figure S2). Conversely, leading cells in hep^{r75} mutants did not show any migratory activity (Martín-Blanco et al., 2000). Hence, the JNK pathway regulates not only the adhesive properties of PS cells, but also their motility.

In summary, the JNK signaling cascade participates in four key steps in the process of disc eversion: (1) the expression of *puc* in PS cells; (2) the apposition of PS and larval cells; (3) the regulation of the adhesive and motile properties of PS cells as they undergo PEMT; and (4) the maintenance of the adhesion between the larval and imaginal tissue (Martín-Blanco et al., 2000).

Discussion

The Eversion of Imaginal Discs

In *Drosophila*, within the first 5 hr after puparium formation, the precursors of the adult structures evert. Multiple evidences show that eversion is mediated by actin microfilaments contraction (Mandaron and Sengel, 1973), which modulate a general change of morphology of PS and larval cells driving the inside-out eversion of the disc. Several observations, however, suggest that other morphogenetic mechanisms are also involved.

First, an imaginal disc is a rigidly determined primordium, which allows the construction of fate maps. Surprisingly, peripodial fate maps of *Calliphora*, a related diptera, show that adjacent territories develop into nonadjacent adult pleural structures (Sprey and Oldenhave, 1974), suggesting that the peripodial layer splits during metamorphosis.

Second, PS cells expressing *puc* relocate during eversion to the leading front (Figure 1). Thus, intercalation of PS cells appears to be concurrent to eversion (Figure 4).

Third, pupal serial sectioning shows that, at eversion, imaginal discs appose to the larval epidermis through their peripodial side (Figure 2). Just before eversion, PS cells lose their basal lamina and detach from the extracellular matrix.

Fourth and finally, preceding disc eversion, in vivo time-lapse reveals the opening of larval/peripodial gaps, which are the outcome of the invasive behavior and planar intercalation (PEMT) of PS cells (Figures 3 and 4).

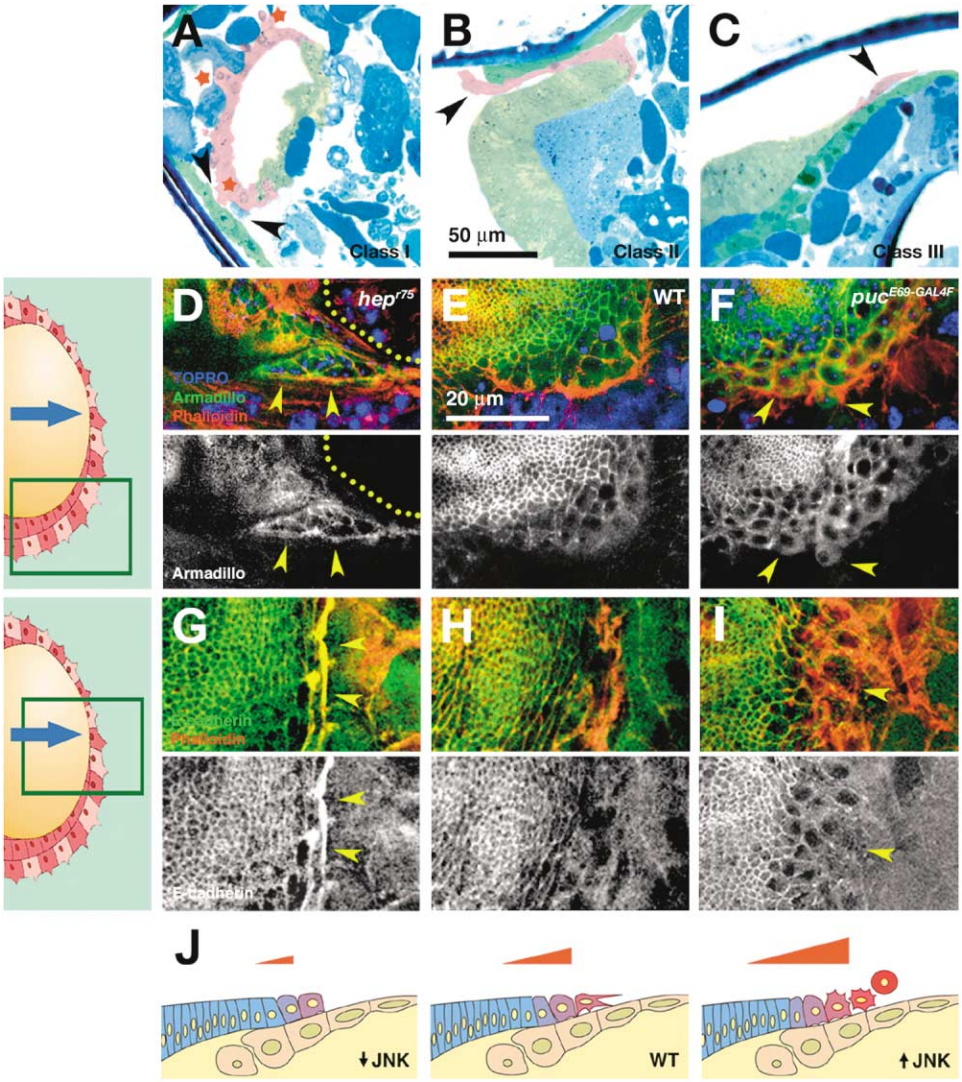

Figure 6. JNK Signaling Regulates the Extent of the Transformation of Peripodial Cells

(A–C) Phenotypic defects of hypomorphic *hep*^{r75} mutants at 6 hr APF. Pupae sagittal sections are color-coded as in Figure 2.

(A) Class I phenotype pupa showing the lack of apposition of PS and larval cells (arrowheads) and no disc eversion. The imaginal epithelium has not folded and the PS cells are undergoing apoptosis (stars).

(B) Class II phenotype pupa with half-everted discs (apposition has taken place). Peripodial-led imaginal spreading does not proceed and PS leading front cells lose their adhesion to the larval tissue (arrowhead).

(C) Discs have everted in a class III pupa and disc spreading has initiated. The leading front cells, however, detach and cannot complete disc fusion (arrowhead).

(D–I) Arm ([D–F], green and lower panel) and DE-cadherin ([G–I], green and lower panel) localization in the leading front of *hep*^{r75} (D, G), wild-type (E, H), and *puc*$^{E69\text{-}F\ GAL4}$ (F, I) pupae. (E and H) In a wild-type condition, Arm and DE-cadherin are eliminated from the cell membranes of imaginal discs leading front cells that disassemble their ZAs and accumulate filamentous actin (phalloidin in red). (D and G) In class II *hep*^{r75} mutant pupae, the free edge membranes of the leading front cells (arrowheads) retain a high concentration of Arm and DE-cadherin. The discs epithelia do not spread and detach from the larval epidermis. Dotted yellow line in (D) delineates the disc detached edge. (F and I) In *puc*$^{E69\text{-}F\ GAL4}$ mutant pupae, with abnormally high levels of JNK activity (see Supplemental Figure S2), Arm and DE-cadherin are excluded from the membrane in a very high number of cells away from the leading front. Many cells round up and ultimately escape from the epithelium. Confocal images correspond to equivalent regions of the posterior half of the left hemithorax of a 4.5 hr APF pupae. Nuclei are shown in blue (TOPRO). Actin (phalloidin) staining is shown in red.

Insets in left panel diagrams indicate the position and orientation of (D)–(I) images at the leading edge of expanding discs.

(J) Wild-type PS cells undergo a pseudo-epithelial-mesenchymal transition during the eversion and closure of imaginal discs. They lose their apico-basal polarity, exhibit high cytoskeleton activity, and become motile and invasive. A reduction of JNK activity (*hep*) prevents these changes. In contrast, increased JNK activity, as in *puc* mutants, results in an extreme loss of epithelial characters that causes cells to round up and detach (see Supplemental Figure S2).

Table 1. Phenotypic Progression after Overexpression of Puc at Larval Stages

	Heat Shock (Hours before Puparium Formation)										
	0–12		12–24		24–36		36–48		48–60		
Wild-type	46	(73,0)	2	(8)	0	(0)	0	(0)	0	(0)	25°C
Class III	5	(7,9)	6	(24)	3	(16,7)	2	(5,6)	0	(0)	
Class II	10	(15,9)	7	(28)	4	(22,2)	10	(27,8)	0	(0)	
Class I	2	(3,2)	10	(40)	11	(61,1)	24	(66,7)	43	(100)	
TOTAL	63		25		19		36		43		
Wild-type	40	(59,7)	0	(0)	0	(0)	0	(0)	0	(0)	29°C
Class III	6	(9,0)	6	(19,4)	4	(8,7)	1	(1,1)	0	(0)	
Class II	9	(13,4)	8	(25,8)	7	(15,2)	6	(6,5)	0	(0)	
Class I	12	(17,9)	17	(54,8)	35	(76,1)	85	(92,4)	24	(100)	
TOTAL	67		31		46		92		24		
Wild-type	28	(100)	37	(78,7)	30	(40,5)	3	(6,3)	0	(0)	25°C
Class III	0	(0)	3	(6,4)	24	(32,4)	8	(16,7)	16	(43,2)	puc
Class II	0	(0)	7	(14,9)	20	(27,0)	25	(52,1)	18	(48,6)	
Class I	0	(0)	0	(0)	0	(0)	12	(25)	3	(8,1)	
TOTAL	28		47		74		48		37		
Wild-type	10	(52,6)	0	(0)	0	(0)	0	(0)	0	(0)	29°C
Class III	9	(47,4)	24	(70,6)	17	(45,9)	15	(40,5)	0	(0)	puc
Class II	0	(0)	5	(14,7)	10	(27,0)	8	(21,6)	4	(26,7)	
Class I	0	(0)	5	(14,7)	10	(27,0)	14	(37,8)	11	(73,3)	
TOTAL	19		34		37		37		15		

Overexpression of Puc at different times before puparium formation. Flies were cultured at the indicated temperatures and the different phenotypes were scored at 6 ± 1 hr APF. Phenotypes are stronger at 29°C and are partially reverted in the presence of a single copy of the puc^{E69} allele. For clones induced at 48–60 hr before puparium formation, 100% of the animals show class I phenotype (complete failure of eversion). Late induction of Puc overexpression leads to weaker phenotypes (class II and class III) or wt flies. Figures in parentheses correspond to percentages. Coded shading colors indicate percentage of individuals in each phenotypic class: 100, 60% gray; 80–100, 50% gray; 60–80, 40% gray; 40–60, 30% gray; 20–40, 20% gray; 0–20, 10% gray; 0, white.

In summary, the evagination of imaginal disc can be divided into the following sequential steps: (1) an overall positional change of the imaginal discs leading to the confrontation and apposition of the PS and the larval epidermis; (2) a regulated modulation (PEMT) of PS cells, which involves the downregulation of their cell-cell adhesion systems and allows them to move into their local neighborhood and invade the larval epithelium; (3) the fenestration of the peripodial/larval bilayer and the formation of an unbound peripodial leading front, which will direct imaginal spreading by planar cell intercalation; and (4) a bulging of the imaginal tissue (Figure 7B).

Once the hole is opened, the planar intercalation of PS cells ensures that, first in the hole and later in the leading front, all four dorsal, ventral, anterior, and posterior compartments of the wing disc are represented. This mechanism also guarantees the maintenance of a continuous epithelial barrier.

Pseudo-Epithelial-Mesenchymal Transition of Peripodial Cells

The loss of epithelial phenotype is a common mechanism involved in many developmental processes. Epithelial cells lose their polarity, disrupt cell-cell interactions, and dissociate from the extracellular matrix (reviewed in Savagner, 2001). Four nonexclusive mechanisms could mediate dissociation: (1) transcriptional downregulation of adhesion components, (2) posttranslational regulation (phosphorylation, ubiquitination), resulting in the destabilization of adhesion structures, (3) downregulation of maintenance signaling pathways, and (4) active degradation of adhesion structural components.

At disc eversion, PS cells disrupt their ZA and lose their basal membrane (Figure 5). They become highly motile and display a dramatic cytoskeletal reorganization. Their actin subcortical mesh is dissociated and show extensive cell ruffling, filopodia, and lamellipodia (Figure 4). This acquisition of mesenchymal properties is achieved through the relocalization of ZA (DE-cadherin and Arm) and septate junction (Coracle and Disc Large) components from the cell membrane to the cytoskeleton. Thus, destabilization of cell-cell adhesion appears not to be achieved by direct transcriptional regulation or degradation, but by some JNK-mediated indirect mechanisms.

The full process of peripodial PEMT must be coordinated in vivo and locally activated. A hormone (ecdysone) input could be a plausible triggering event. High levels of ecdysone direct the onset of eversion of discs in vitro (Milner, 1977), and various genes of the ecdysone regulatory cascade are expressed in the PE (see Fristrom and Fristrom, 1993). In fact, animal mutants for the EcR-B1 isoform of the ecdysone receptor fail to evert their discs (Bender et al., 1997). Still, it remains to be

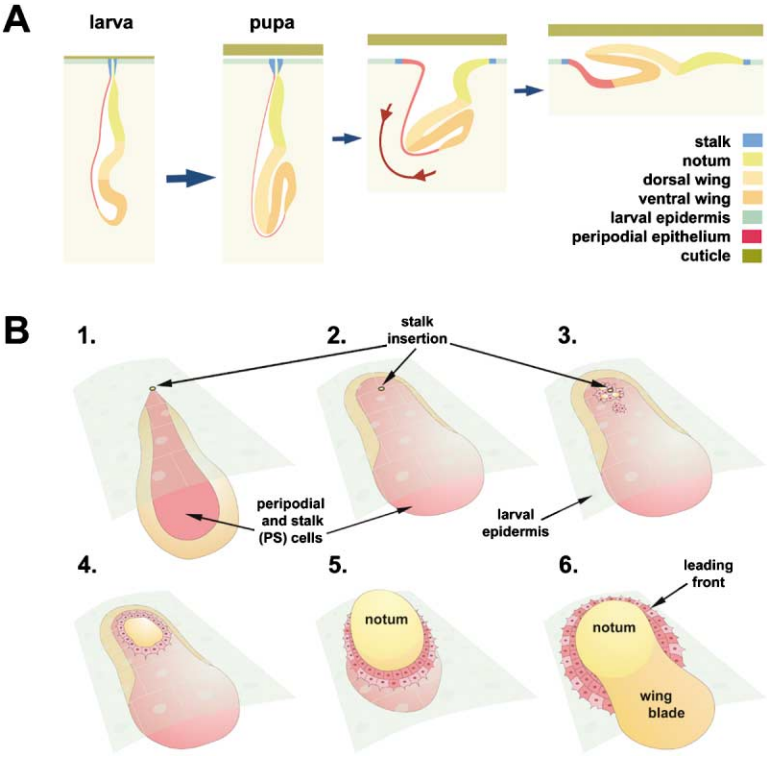

Figure 7. Imaginal Disc Eversion

(A) Inside-out reversion model (2D reconstruction) of imaginal discs eversion (Fristrom and Fristrom, 1993). The movement of the appendages to the outside of the larval epidermis was thought to occur through widened disc stalks by the contraction of an intact peripodial epithelium. Peripodial cell shape changes were suggested to be sufficient for imaginal disc eversion. Time lapse and ultrastructural analysis, in line with early alternative models, suggest that, besides cell shape changes, the rupture of the peripodial epithelium is essential for disc eversion (see below).

(B) Schematic time course of the main events in the eversion of imaginal wing discs by peripodial/larval perforation (3D reconstruction). (1) Discs hang from a stalk into the body cavity during larval stages. (2) During the first hours of metamorphosis, PS cells appose to the larval epidermis. (3) Between 3.5 and 4 hr APF, PS cells invade the larval epidermis and replace larval cells on the pupal surface at different points. Soon after, loss of adhesion among PE cells opens several holes in the disc epithelium. (4) The initial holes coalesce into a single perforation. (5) This hole widens by intercalation of new PS cells at the edge. (6) As widening of the hole proceeds, the wing disc is extruded. At the end of eversion, the PS has become a stripe of proximal cells that surrounds the disc. This stripe of cells constitutes the leading front guiding the spreading of the disc over the larval epithelium. The fusion of the wing imaginal discs at the dorsal midline is accomplished at 5.5 hr APF.

Notum, wing territories, and the peripodial and the larval epithelium in both diagrams have been coded with equivalent colors.

established if ecdysone signaling might control cell-cell adhesion and cytoskeletal changes.

The Leading Front

PS cells intercalate during eversion and become the marginal cells of the migrating epithelia. This planar intercalation is reminiscent of *Xenopus* mesoderm "convergent extension" by medio-lateral cell intercalation (Keller, 2002) and epithelial planar intercalation during *Drosophila* germ band extension (Irvine and Wieschaus, 1994).

At the leading front, PS cells maintain loose contact with their neighbors, extending lamellipodia and filopodia in the direction of movement. This active movement at the leading front evokes chick epiboly (Arendt and Nubler-Jung, 1999). Both movements require the presence of a tense, unbroken epithelium on which to adhere and spread. Migration would exert a tensile, compressive force. To gain traction, PS cells must orientate the distribution of new contacts to their leading edge and break contacts at their trailing edge. What are the signals leading these activities? How are they detected? And through which mechanisms are they transduced to result in a directed movement? Some insights may be obtained from studies on the migration of oocyte border cells. *Drosophila* border cells are a specialized group of cells that exit the somatic follicle epithelium and migrate between the nurse cells toward the anterior pole of the oocyte. The border cells extend long filopodia, which play a role in signal sensing and movement. This process, as disc eversion, is directed by DE-cadherin-dependent interactions (Montell, 2003). PVF1, a ligand for the PDGF/VEGF receptor, directs the anterior and dorsal movements of border cells (McDonald et al., 2003). Signaling through PDGF/VEGF receptor requires Myoblast city (Mbc), the *Drosophila* Dock180, which modulates Rac activity (Duchek et al., 2001). Interestingly, *mbc* mutants show dorsal closure defects, suggesting a role for Mbc in PS cell migration that remains to be explored.

Multiple Roles of the JNK Cascade

In *Drosophila*, the JNK pathway is known as a mediator of embryonic dorsal closure. Impaired JNK signaling in the developing embryo is associated with failure to generate actin-based protrusions by leading edge cells (reviewed in Martín-Blanco and Knust, 2001).

At the onset of eversion, the activity of the JNK signaling pathway is necessary for the apposition of PS and larval cells (Figure 2). JNK signaling couples the mechanical deformation of discs, mediated by cell shape changes of PS cells and their presentation and adhesion to the larval epidermal layer through their basal surfaces. How JNK activity controls PS cells shape and contractility, and which genes participate in peripodial apposition, is unclear. A recent SAGE study has identified numerous genes that respond transcriptionally to alterations in JNK signaling (Jasper et al., 2001). Among the genes upregulated by activation of the JNK cascade is *chickadee* (*chic*), which encodes *Drosophila* Profilin (Cooley et al., 1992). Profilin is an actin binding protein involved in F-actin polymerization and regulation of cytoskeleton

dynamics (Yang et al., 2000). *chic* mutant embryos present dorsal closure defects and show genetic interactions with *hep*. Still, the role of *chic* in peripodial contractility or in the spreading of leading front cells remains to be determined.

Following disc apposition to the larval tissue, the JNK cascade directs the acquisition by PS cells of a pseudomesenchymal phenotype (Figure 6). PS cells alter their DE-cadherin, Arm (Figure 2), APC, P-Tyr, and Dα-catenin (data not shown) expression, invade the larval tissue, and intercalate at the leading front. The JNK pathway regulates the loss of both cell-cell contacts and the PS cell motile activity (Figures 4 and 5). A set of proteins that could participate in the JNK activity-mediated PEMT are the small GTPases of the Rho family. Rho1 accumulates at sites of DE-cadherin localization, and in zygotic *Rho1* mutant embryos, DE-cadherin is diffusely distributed across the cell (Magie et al., 2002). Moreover, all *Drosophila* Rho family proteins DRac1, DRac2, Mtl, Dcdc42, and Rho1 appear to participate in dorsal closure (reviewed in Harden, 2002).

Finally, the JNK activity is both necessary and sufficient for *puc* expression. Puc could have two non-mutually exclusive potential roles: it could either act as a buffer for the fine-tuning and/or stabilization of JNK activity or, alternatively, help to repress JNK activity when it is no longer required. How leading front cells hold the equilibrium between motility and adhesion and how adherens junctions turnover is regulated in response to JNK is, however, still unknown.

Our results suggest that imaginal disc eversion should not be regarded as a simple outcome of the activation of JNK signaling, but rather as an output of the integration of several processes including planar polarization, cytoskeletal activity, and gene expression.

Epithelial Perforation

The fenestration of the peripodial/larval bilayer during imaginal disc eversion is suggestive of other developmental processes (e.g., the formation of the pharyngeal fissures, or the aperture of the oral, urogenital, and anal membranes in chordates) where the perforation of transient epithelia creates a communication between chambers and the external environment (reviewed in Manni et al., 2002). Although the process of fenestration is extremely common, the steps that lead to the rearrangement of epithelial cells to create a hole remain unknown. Following the cellular analysis of imaginal disc eversion, it would be of interest to determine the putative roles of the JNK and other related cascades during epithelial perforation in chordates. These studies will uncover similarities and differences that may be crucial for our understanding of this basic developmental process.

Experimental Procedures

Fly Strains

The following strains were used in this study: UAS-Puc2A (Martín-Blanco et al., 1998), puc^{E69} (Ring and Martínez Arias, 1993), puc^{B48R23} (Martín-Blanco et al., 1998), hep^{r75} (Glise et al., 1995), UAS-GFP.Y (Yeh et al., 1995), AyGAL4 UAS-GFP.S65T (Ito et al., 1997), Ub-DE-Cadherin-GFP (Oda and Tsukita, 2001), UAS-FLP1.D (Campbell and Tomlinson, 1998), and UAS-y.C (Calleja et al., 1996).

For the lineage analysis in the peripodial epithelium, clones were induced in *y w* hsp70-flp; AyGAL4 UAS-GFP.S65T; puc^{E69}/SM6a-TM6B (Ito et al., 1997) and *y w* hsp70-flp; P{2xGFP} FRT40A/FRT40A at 24–48 after egg laying by heat shock treatment at 37°C for 7 and 30 min, respectively.

For ubiquitous overexpression of Puc, *y w* hsp70-flp; AyGAL4 UAS-GFP.S65T; TM2/SM6a-TM6B and *y w* hsp70-flp; AyGAL4 UAS-GFP.S65T; puc^{E69}/SM6A-TM6B flies were crossed to UAS-Puc2A flies and larvae heat shocked at 37°C for 1 hr.

puckered-GAL4 Lines

Several lines expressing GAL4 in the same pattern as *puc* were obtained by substitution of the [lacZ, ry^+] insertion in puc^{E69} for a [GAL4, w^+] insertion (Sepp and Auld, 1999). 500 puc^{E69} males, bearing a GAL4 insertion in the X chromosome and a transposase source, were crossed in mass to 1000 *w; If*/CyO; MKRS/TM6B females. 18 males selected by rescue of the *w* mutation were recovered and independent lines were established. 11 out of these 18 lines were inserted in the same position as the original P element, puc^{E69}, and expressed GAL4 in a pattern resembling that of *puc*. In homozygosis, five lines apparently produced wt but unfertile flies ($puc^{E69\text{-}A}$, $puc^{E69\text{-}G}$, $puc^{E69\text{-}H}$, $puc^{E69\text{-}I}$, and $puc^{E69\text{-}K}$), three lines were semiviable mutants with defects in the closure of imaginal discs ($puc^{E69\text{-}F}$, $puc^{E69\text{-}M}$, $puc^{E69\text{-}Q}$), and the remaining three were embryonic lethals ($puc^{E69\text{-}C}$, $puc^{E69\text{-}E}$, $puc^{E69\text{-}S}$). All of these 11 lines are *puc* loss-of-function alleles and fail to complement puc^{B48R23}, puc^{E69}, and a deficiency that uncovers the *puc* locus (Df(3R)p712). $puc^{E69\text{-}I}$ was chosen for imaging of the wt process and $puc^{E69\text{-}F}$ for functional studies.

Inmunocytochemistry

Dissected pupae were stained by standard methods. Specimens were fixed for 20 min in a 4% paraformaldehyde solution in PBT (PBS/0.1% Tween 20) and inmunostained in PBT-BSA (PBT/0.3%BSA) with mouse anti-Armadillo (Arm) (Hybridoma Bank), rat anti-DE-cadherin (Oda et al., 1994), guinea pig anti-coracle (Fehon et al., 1994), mouse anti-β-gal (Promega), rabbit anti-β-gal (Cappel) antibodies. Alexa Fluor-488, -546 (Molecular Probes), or Cy5 (Jackson InmunoResearch) conjugated secondary antibodies were used. F-actin stainings were performed with Texas red-coupled phalloidin (Sigma). Cell nuclei were stained with DAPI or To-Pro-3 iodide (TOPRO) (Molecular Probes). Pupae were mounted in Vectashield (Vector Laboratories).

Semithin and Ultrathin Sections

Anterior halves of pupae were semidissected after removing the fat attached to the pupal case and fixed in 4% glutaraldehyde in phosphate buffer for 30 min. Specimens were postfixed for 30 min in a mixture of 2% glutaraldehyde and 1% osmium tetroxide and 30 additional minutes in 2% osmium tetroxide, both in phosphate buffer on ice and contrasted with 2% uranyl acetate in water. Pupae were embedded in araldite after dehydration with graded ethanol and acetone. Semithin sections (2.5 μm) were stained with toluidine blue. Ultrathin sections for electron microscopy (50–100 nm) were postcontrasted with uranyl acetate and lead citrate.

Movies

Epifluorescence was used to shoot movies through the pupal case by closely adhering the appropriate region of the pupa to a cover glass with a drop of Voltalef 10S oil. A SpotII CCD camera was used in an upright Zeiss Axioplan Imaging microscope. The room was maintained at 25°C. An image was taken every 30 s for Movies S1 to S3 and every 15 s for Movie S4 using Metamorph software.

Acknowledgments

The authors would like to acknowledge the different groups that have provided reagents and fly stocks to perform this work. Special thanks to E. Knust, C. Antoniewski, R. Leborgne, and F. Schweisguth who hosted JCPP at different stages of this project. We also would like to thank J. Capdevila, J.C. Izpisua-Belmonte, T. Kornberg, M. Affolter, F. Giraldez, and the anonymous reviewers for comments on the manuscript. J.C.P.-P. was supported by a PhD Studentship of the Comunidad Autónoma de Madrid. This work was funded by grants of the DGICYT to A.G.-B. and E.M.-B. and FIS to A.G.-B.

A.G.-B. acknowledges the institutional support of the Fundación Ramón Areces to the CBMSO. E.M.-B. wants to thank the encouragement of Engràcia Querol during the writing of the manuscript.

Received: January 20, 2004
Revised: May 20, 2004
Accepted: July 12, 2004
Published: September 13, 2004

References

Agnes, F., Suzanne, M., and Noselli, S. (1999). The *Drosophila* JNK pathway controls the morphogenesis of imaginal discs during metamorphosis. Development *126*, 5453–5462.

Arendt, D., and Nubler-Jung, K. (1999). Rearranging gastrulation in the name of yolk: evolution of gastrulation in yolk-rich amniote eggs. Mech. Dev. *81*, 3–22.

Auerbach, Ch. (1936). The development of the legs, wings and halteres in wild type and some mutant strains of *Drosophila melanogaster*. Trans. R. Soc. Edinb. *58*, 114–119.

Bender, M., Imam, F.B., Talbot, W.S., Ganetzky, B., and Hogness, D.S. (1997). *Drosophila* ecdysone receptor mutations reveal functional differences among receptor isoforms. Cell *91*, 777–788.

Calleja, M., Moreno, E., Pelaz, S., and Morata, G. (1996). Visualization of gene expression in living adult *Drosophila*. Science *274*, 252–255.

Campbell, G., and Tomlinson, A. (1998). The roles of the homeobox genes *aristaless* and *Distal-less* in patterning the legs and wings of *Drosophila*. Development *125*, 4483–4493.

Cooley, L., Verheyen, E., and Ayers, K. (1992). *chickadee* encodes a profilin required for intercellular cytoplasm transport during *Drosophila* oogenesis. Cell *69*, 173–184.

Duchek, P., Somogyi, K., Jekely, G., Beccari, S., and Rorth, P. (2001). Guidance of cell migration by the *Drosophila* PDGF/VEGF receptor. Cell *107*, 17–26.

Fehon, R.G., Dawson, I.A., and Artavanis-Tsakonas, S. (1994). A *Drosophila* homologue of membrane-skeleton protein 4.1 is associated with septate junctions and is encoded by the coracle gene. Development *120*, 545–557.

Fristrom, D., and Fristrom, J.W. (1993). The metamorphic development of the adult epidermis. In The Development of *Drosophila melanogaster*, M. Bate and A. Martínez-Arias, eds. (New York: Cold Spring Harbor Laboratory Press), pp. 843–897.

Glise, B., Bourbon, H., and Noselli, S. (1995). *hemipterous* encodes a novel *Drosophila* MAP kinase kinase, required for epithelial cell sheet movement. Cell *83*, 451–461.

Harden, N. (2002). Signaling pathways directing the movement and fusion of epithelial sheets: lessons from dorsal closure in *Drosophila*. Differentiation *70*, 181–203.

Irvine, K.D., and Wieschaus, E. (1994). Cell intercalation during *Drosophila* germband extension and its regulation by pair-rule segmentation genes. Development *120*, 827–841.

Ito, K., Awano, W., Suzuki, K., Hiromi, Y., and Yamamoto, D. (1997). The *Drosophila mushroom body* is a quadruple structure of clonal units each of which contains a virtually identical set of neurons and glial cells. Development *124*, 761–771.

Jasper, H., Benes, V., Schwager, C., Sauer, S., Clauder-Munster, S., Ansorge, W., and Bohmann, D. (2001). The genomic response of the *Drosophila* embryo to JNK signaling. Dev. Cell *1*, 579–586.

Keller, R. (2002). Shaping the vertebrate body plan by polarized embryonic cell movements. Science *298*, 1950–1954.

Knust, E., and Bossinger, O. (2002). Composition and formation of intercellular junctions in epithelial cells. Science *298*, 1955–1959.

Magie, C.R., Pinto-Santini, D., and Parkhurst, S.M. (2002). Rho1 interacts with p120ctn and alpha-catenin, and regulates cadherin-based adherens junction components in *Drosophila*. Development *129*, 3771–3782.

Mandaron, P., and Guillermet, C. (1978). Analyse microcinématographique de l'evagination des disques d'aile et de patte de *Drosophile* cultivés *in vitro*. C R Acad. Sci. III *D287*, 257–260.

Mandaron, P., and Sengel, P. (1973). Effect of cytochalasin B on the evagination *in vitro* of leg imaginal discs. Dev. Biol. *32*, 201–207.

Manni, L., Lane, N.J., Zaniolo, G., and Burighel, P. (2002). Cell reorganization during epithelial fusion and perforation: the case of ascidian branchial fissures. Dev. Dyn. *224*, 303–313.

Martín-Blanco, E. (1997). Regulation of cell differentiation by the *Drosophila* Jun kinase cascade. Curr. Opin. Genet. Dev. *7*, 666–671.

Martín-Blanco, E., and Knust, E. (2001). Epithelial morphogenesis: filopodia at work. Curr. Biol. *11*, R28–R31.

Martín-Blanco, E., Gampel, A., Ring, J., Virdee, K., Kirov, N., Tolkovsky, A.M., and Martínez-Arias, A. (1998). *puckered* encodes a phosphatase that mediates a feedback loop regulating JNK activity during dorsal closure in *Drosophila*. Genes Dev. *12*, 557–570.

Martín-Blanco, E., Pastor-Pareja, J.C., and Garcia-Bellido, A. (2000). JNK and *decapentaplegic* signaling control adhesiveness and cytoskeleton dynamics during thorax closure in *Drosophila*. Proc. Natl. Acad. Sci. USA *97*, 7888–7893.

McDonald, J.A., Pinheiro, E.M., and Montell, D.J. (2003). *PVF1*, a PDGF/VEGF homolog, is sufficient to guide border cells and interacts genetically with *Taiman*. Development *130*, 3469–3478.

Milner, M.J. (1977). The eversion and differentiation of *Drosophila melanogaster* leg and wing imaginal discs cultured in vitro with an optimal concentration of beta-ecdysone. J. Embryol. Exp. Morphol. *37*, 105–117.

Milner, M.J., Bleasby, A.J., and Kelly, S.L. (1984). The role of the peripodial membrane of leg and wing imaginal disks of *Drosophila-melanogaster* during evagination and differentiation *in vitro*. Rouxs Arch. Dev. Biol. *193*, 180–186.

Montell, D.J. (2003). Border-cell migration: the race is on. Nat. Rev. Mol. Cell Biol. *4*, 13–24.

Noselli, S. (1998). JNK signaling and morphogenesis in *Drosophila*. Trends Genet. *14*, 33–38.

Noselli, S., and Agnes, F. (1999). Roles of the JNK signaling pathway in *Drosophila* morphogenesis. Curr. Opin. Genet. Dev. *9*, 466–472.

Oda, H., and Tsukita, S. (2001). Real-time imaging of cell-cell adherens junctions reveals that *Drosophila* mesoderm invagination begins with two phases of apical constriction of cells. J. Cell Sci. *114*, 493–501.

Oda, H., Uemura, T., Harada, Y., Iwai, Y., and Takeichi, M. (1994). A *Drosophila* homolog of cadherin associated with armadillo and essential for embryonic cell-cell adhesion. Dev. Biol. *165*, 716–726.

Poodry, C.A., and Schneiderman, H.A. (1970). The ultrastructure of the developing leg of *Drosophila melanogaster*. Rouxs Arch. Dev. Biol. *166*, 1–44.

Resino, J., Salama-Cohen, P., and Garcia-Bellido, A. (2002). Determining the role of patterned cell proliferation in the shape and size of the *Drosophila* wing. Proc. Natl. Acad. Sci. USA *99*, 7502–7507.

Riesgo-Escovar, J.R., Jenni, M., Fritz, A., and Hafen, E. (1996). The *Drosophila* Jun-N-terminal kinase is required for cell morphogenesis but not for DJun-dependent cell fate specification in the eye. Genes Dev. *10*, 2759–2768.

Ring, J.M., and Martínez Arias, A. (1993). *puckered*, a gene involved in position-specific cell differentiation in the dorsal epidermis of the *Drosophila* larva. Development (*Suppl*.), 251–259.

Savagner, P. (2001). Leaving the neighborhood: molecular mechanisms involved during epithelial-mesenchymal transition. Bioessays *23*, 912–923.

Sepp, K.J., and Auld, V.J. (1999). Conversion of lacZ enhancer trap lines to GAL4 lines using targeted transposition in *Drosophila melanogaster*. Genetics *151*, 1093–1101.

Sprey, T.E., and Oldenhave, M. (1974). A detailed organ map of the wing disk of *Calliphora erytrocephala*. Neth. J. Zool. *24*, 291–310.

Suzanne, M., Perrimon, N., and Noselli, S. (2001). The *Drosophila* JNK pathway controls the morphogenesis of the egg dorsal appendages and micropyle. Dev. Biol. *237*, 282–294.

Tateno, M., Nishida, Y., and Adachi-Yamada, T. (2000). Regulation of JNK by Src during *Drosophila* development. Science *287*, 324–327.

Usui, K., and Simpson, P. (2000). Cellular basis of the dynamic

behavior of the imaginal thoracic discs during *Drosophila* metamorphosis. Dev. Biol. *225*, 13–25.

Waddington, C.H. (1941). The genetic control of wing development in *Drosophila*. J. Genet. *41*, 75–139.

Wolpert, L., Beddington, R., Jessell, T., Lawrence, P., Meyerowitz, E., and Smith, J. (2002). Principles of Development (London: Oxford University Press).

Yang, C., Huang, M., DeBiasio, J., Pring, M., Joyce, M., Miki, H., Takenawa, T., and Zigmond, S.H. (2000). Profilin enhances Cdc42-induced nucleation of actin polymerization. J. Cell Biol. *150*, 1001–1012.

Yeh, E., Gustafson, K., and Boulianne, G.L. (1995). Green fluorescent protein as a vital marker and reporter of gene expression in *Drosophila*. Proc. Natl. Acad. Sci. USA *92*, 7036–7040.

Zeitlinger, J., and Bohmann, D. (1999). Thorax closure in *Drosophila*: involvement of Fos and the JNK pathway. Development *126*, 3947–3956.

Zeitlinger, J., Kockel, L., Peverali, F.A., Jackson, D.B., Mlodzik, M., and Bohmann, D. (1997). Defective dorsal closure and loss of epidermal *decapentaplegic* expression in *Drosophila fos* mutants. EMBO J. *16*, 7393–7401.